Influence of a Novel β-Nucleating Agent on the Structure, Morphology, and Nonisothermal Crystallization Behavior of Isotactic Polypropylene

Wenchang Xiao,[1] Peiyi Wu,[1] Jiachun Feng,[1] Riyuan Yao[2]

[1]*Key Laboratory of Molecular Engineering of Polymers of Ministry of Education, Department of Macromolecular Science, Fudan University, Laboratory of Advanced Materials, Shanghai 200433, People's Republic of China*
[2]*Yangzhou Petrochemical Factory, Yangzhou 225200, People's Republic of China*

Received 25 May 2008; accepted 9 August 2008
DOI 10.1002/app.29139
Published online 17 October 2008 in Wiley InterScience (www.interscience.wiley.com).

ABSTRACT: The crystalline structure, morphology, and nonisothermal crystallization behavior of isotactic polypropylene (iPP) with and without a novel rare earth-containing β-nucleating agent (WBG) were investigated with wide-angle X-ray diffraction, polar optical microscopy, and differential scanning calorimetry. WBG could induce the formation of the β form, and a higher proportion of the β form could be obtained by the combined effect of the optimum WBG concentration and a lower cooling rate. The content of the β form could reach more than 0.90 in a 0.08 wt % WBG nucleated sample at cooling rates lower than 5°C/min. Polar optical microscopy showed that WBG led to substantial changes in both the morphological development and crystallization process of iPP. At all the studied cooling rates, the temperature at which the maximum rate of crystallization occurred was increased by 8–11°C in the presence of the nucleating agent. An analysis of the nonisothermal crystallization kinetics also revealed that the introduction of WBG significantly shortened both the apparent incubation period for crystallization and the overall crystallization time. © 2008 Wiley Periodicals, Inc. J Appl Polym Sci 111: 1076–1085, 2009

Key words: crystallization; nucleation; poly(propylene) (PP)

INTRODUCTION

Isotactic polypropylene (iPP) is one of the most widely used thermoplastic materials because of its favorable price/performance ratio and the ease of modifying it as a basic material. It is a typical polymorphic material with several basic crystalline forms (α, β, γ, etc.).[1–3] Generally, the α form predominates under ordinary conditions of solidification from the melt, and only under some special conditions can other forms predominate. Among these crystalline forms, the β form usually shows improved elongation at break and better impact strength in comparison with the other forms,[4–11] and so it has received much attention in scientific research and industrial applications.

At present, several methods, including the addition of β-nucleating agents,[4,7] directional crystallization in certain temperature gradients,[12,13] and subjection to shear,[14,15] are used to increase the proportion of the β form in iPP. From a practical point of view, the addition of β-nucleating agents to iPP is still the most effective and accessible way of obtaining iPP with a high content of the β form. Thus, the development of various β-nucleating agents has attracted much attention.[4,7,16–25] Up to now, there have been mainly three classes of compounds in widely used β-nucleating agents:[4,7] a minority of aromatic ring compounds, such as γ-quinacridone (Dye Permanent Red E3B) and triphenodithiazine;[11,16] certain group IIA metal salts or their mixtures with some specific dicarboxylic acids, such as calcium salt of imido acids and compounds of calcium stearate and pimelic acid;[17–20] and some substituted aromatic bisamides, including mainly *N,N′*-dicyclohexylterephthalamide and *N,N*-dicyclohexyl-2,6-naphthalene dicarboxamide.[21–25] Hence, the development of an effective, cheap, and accessible β-nucleating agent remains an essential topic in the field of composite material research.

Correspondence to: J. Feng (jcfeng@fudan.edu.cn).
Contract grant sponsor: National Natural Science Foundation of China; contract grant number: 50673021.
Contract grant sponsor: National Basic Research Program of China; contract grant number: G2005CB623803.
Contract grant sponsor: Hi-Tech Research & Development Program of China; contract grant number: 2007AA03Z450.
Contract grant sponsor: Natural Science Foundation of Shanghai; contract grant number: 06ZR14007.
Contract grant sponsor: Guangdong Province & National Ministry of Education Special Funds; contract grant number: 2007A090302091.

We found early on that, despite having low β-nucleating activity, some mixtures consisting of rare earth compounds and some mineral additives could induce β-form formation.[26,27] We surmised that the true β-iPP nucleating agent in these systems might be some binuclear complexes of calcium and rare earth elements with some ligands. On the basis of this idea, we synthesized a series of heteronuclear dimetal complexes of lanthanum and calcium with some specific ligands that had been prepared and applied to commercial β-nucleating agent production (WBG). Our previous study[28] showed that the addition of 0.8 wt % WBG could result in the occurrence of more than 90% β form and a large increase in the crystallization rate of iPP under isothermal conditions. To further understand the nucleation effect of WBG, the crystalline structure, morphology, and nonisothermal crystallization behavior of iPP/WBG systems were investigated with wide-angle X-ray diffraction (WAXD), polar optical microscopy (POM), and differential scanning calorimetry (DSC).

EXPERIMENTAL

Materials

The iPP employed in this work was F401, a product of Yangzi Petrochemical Co. (Sinopec, Nanjing, China); it had a melt flow rate of 2.5 g/10 min (230°C, 2.160 kg), a density of 0.91 g/mL, and a tacticity of 96.5%. Small amounts of antioxidants (Irganox 1010 and Irganox 168) existed in the as-received iPP; therefore, no additional antioxidant was used. The rare earth-containing β-nucleating agent, WBG, was a heteronuclear dimetal complex of lanthanum and calcium with some specific ligands. It was kindly supplied by Guangdong Winner Functional Materials Co., Ltd. (Foshan City, China).

Preparation of the mixtures and samples

Compounding of the iPP granules and WBG white powders was performed by melt blending with a Brabender PLE-651 mixer (Duisberg, Germany). The temperature was fixed at 170°C, and the roller speed was set at 45 rpm. WBG at concentrations of 0.025, 0.04, 0.08, 0.10, 0.12, and 0.15 wt % was added. After a constant value of the torque was obtained, the melted mixture was mixed another 7 min until a homogeneous blend was obtained.

The obtained iPP/WBG mixtures were subsequently molded into 0.4-mm-thick sheets at 190°C in a press under a pressure of 15 MPa for 5 min and then naturally cooled to room temperature. In this case, the natural cooling rate was estimated to be 40–60°C/min in the temperature range of 150–100°C, in which the primary crystallization occurred. Also, a pure iPP sample sheet was prepared with an identical mixing and molding schedule and used as a control. The nucleated iPP, containing 0.08 wt % WBG, is denoted W-008 for convenience.

WAXD

WAXD measurements were performed with a PANalytical X'pert diffractometer (Alemelo, The Netherlands) in a reflection mode with Ni-filtered Cu Kα radiation ($\lambda = 0.154$ nm) with a voltage of 40 kV and a current of 40 mA. Radial scans of the intensity versus the diffraction angle (2θ) were recorded in the region of 5–30°. After the usual correction, the X-ray curves were resolved into contributions of crystalline peaks and amorphous peaks. The overall degree of crystallinity (X_c) of each sample was determined from the peak areas in the region of 10–30°, and the relative proportion of the β form (k_β) in the crystalline part was calculated with the widely accepted empirical equation of Turner-Jones et al.:[29]

$$k_\beta = H(\beta)/[H(\beta) + H(\alpha 1) + H(\alpha 2) + H(\alpha 3)] \quad (1)$$

where $H(\alpha 1)$, $H(\alpha 2)$, and $H(\alpha 3)$ are the intensities of the three α-diffraction peaks (110), (040), and (130), corresponding to 2θ angles at 14.0, 16.8, and 18.6°, respectively, and $H(\beta)$ is the intensity of the strong single β peak (300) at $2\theta = 16.0°$.

Samples for WAXD measurements were cut directly from the obtained 0.4-mm-thick sheets. To investigate the effect of the cooling condition on its crystalline structures, sample W-008 was also melted at 200°C, kept there for 5 min, and then cooled to 40°C at different cooling rates ranging from 2 to 30°C/min with a Linkham THMS600 hot stage (Surrey, England). Then, the as-treated samples were characterized with WAXD.

POM

The spherulitic morphologies of pure iPP and W-008 were observed with an Olympus BX-51 polarized optical microscope (Tokyo, Japan) with a Linkam THMS600 hot stage. The temperature of the hot stage could be kept constant within 0.1°C, and nitrogen gas was purged through the hot stage during measurements. The samples for POM observation were prepared by melting and squeezing into films. These films were kept in the hot stage between two microscope slides, and each sample was heated to 200°C and kept at this temperature for 5 min to erase its thermal history. Samples were subsequently cooled to room temperature at a cooling rate of 20°C/min, and a nonisothermal crystallization process was observed. For comparison, the samples were rapidly cooled to 134°C and maintained until

the completion of crystallization to observe the isothermal crystallization process.

DSC

All the samples for DSC measurements were also cut from 0.4-mm-thick sheets. DSC measurements were performed with a TAQ-100 thermal analysis system (New Castle, DE) in a nitrogen atmosphere. The temperature calibration was performed with indium (peak melting temperature = 156.60°C and initial enthalpy of fusion = 28.45 J/g) as a standard to ensure the reliability of the obtained data. The inaccuracy of the temperature measured here was ±0.05°C. To investigate the β-nucleated selectivity of WBG, iPP and 0.1 wt % WBG nucleated iPP were heated to 210°C and maintained there for 5 min before they were cooled to 100°C at a cooling rate of 10°C/min and subsequently reheated at 10°C/min. The last melting traces were recorded to evaluate the β-nucleated selectivity of WBG. To study the nonisothermal crystallization behavior, 6–9 mg of each sample was first heated to 200°C at a scanning rate of 10°C/min and maintained there for 5 min to diminish the influence of the previous thermal and mechanical history; the samples were then cooled to 40°C at five preset cooling rates of 2, 5, 10, 20, and 30°C/min. The crystallization traces were recorded to study the thermal properties and the nonisothermal crystallization kinetics.

RESULTS AND DISCUSSION

Structure analysis

WAXD examinations were carried out to obtain information about the crystalline structures, and the results are shown in Figure 1. For pure iPP, there are five local maxima at 2θ values of approximately 14.0, 16.8, 18.6, 21.2, and 21.8°, corresponding to the (110), (040), and (130) reflections and overlapping (131) and (111) reflections, which are characteristic peaks of the monoclinic α form. On the contrary, for the patterns of WBG-nucleated iPPs, another peak appears at 2θ = 16.0°, which can be accounted for by the (300) plane of the hexagonal β form. Moreover, this peak is more pronounced as the concentration of WBG increases. These changes clearly indicate that only the α form exists in pure iPP, whereas the addition of WBG can largely induce the formation of the β form in WBG-nucleated samples. X_c and k_β, which were calculated with eq. (1) for iPP with various concentrations of WBG, are shown in Figure 2. Under identical natural cooling conditions, there is no essential difference in X_c for all the samples. However, the value of k_β increases significantly with the WBG concentration: iPP modified by 0.025 wt % WBG is only 29% β form, whereas that value rapidly increases to nearly 80% for iPP nucleated with 0.08 wt % WBG. However, the values of k_β experience no substantial increase with the WBG concentration further increasing. These results imply that the WBG has an optimum concentration (~ 0.08 wt %), and too much WBG provides no more help for inducing the formation of β-iPP.[6,11] Therefore, in this work, we chose a sample containing 0.08 wt % WBG (W-008) for further analysis.

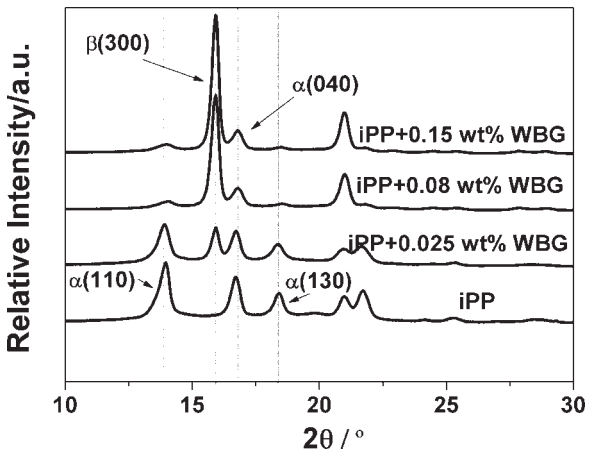

Figure 1 X-ray diffraction patterns of virgin iPP and nucleated iPP.

On the other hand, the crystallization condition is also an important extrinsic parameter influencing the crystalline structures of iPP. In the previous study,[28] we investigated the isothermal crystallization and melting behavior of iPP with and without the nucleating agent WBG. From the melting curves, we evaluated the influence of the isothermal crystallization temperature on the formation of the β form, and we found that the efficiency of WBG was greater at a lower isothermal crystallization temperature among the studied temperatures. This could be explained by the different growth rates of different crystalline forms and the β–α transformation under high crystallization temperatures.[3,30] However, the most practical industrial processing proceeds under nonisothermal conditions; in this study, we employed sample W-008 to investigate the influence of different cooling rates on the final crystalline structures of iPP.

Figure 3 shows the corresponding X-ray diffraction patterns of sample W-008 crystallized under various cooling conditions. For the samples crystallized at cooling rates of 30, 10, 5, and 2°C/min, the k_β values are 0.82, 0.86, 0.90, and 0.91, respectively. Moreover, the value is 0.78 for the W-008 sample crystallized under air-cooling conditions (ca. 40–60°C/min). Obviously, the proportion of the β form can reach more than 90% at lower cooling rates for

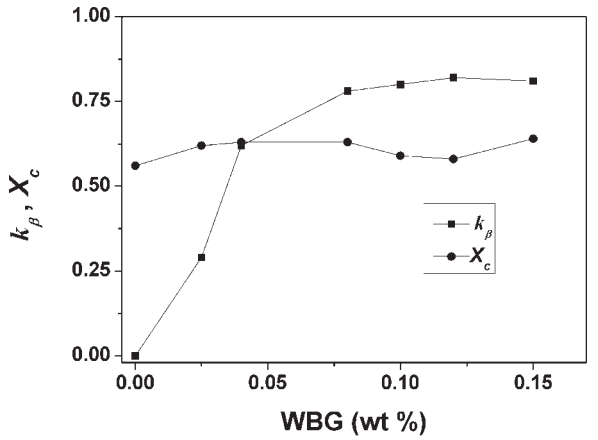

Figure 2 Influence of the WBG concentration on X_c and k_β.

W-008. It can be concluded that the lower the cooling rate is, the higher the proportion of the β form will be. Some research groups[3,20] earlier reported that the amount of the α form could be suppressed if the cooling rate were slowed below 5°C/min, and our results agree very well with those studies. During the nonisothermal crystallization of W-008, when the cooling rate is low, crystallization occurs in a higher temperature region (shown later in Fig. 7) in which the self-nucleation of iPP is difficult to initiate, and the nucleating agent WBG can effectively provide a large number of foreign nuclei to induce the formation of the β form. On the contrary, at a high cooling rate, crystallization occurs in a lower temperature region in which the self-nucleation of iPP is still pronounced, and this can result in a certain amount of the α form. Therefore, a higher proportion of the β form can be obtained by the combined effect of an optimal nucleating agent concentration and a lower cooling rate.

Morphological development

The intense effect of WBG on the structure and morphology of iPP is also reflected in the morphological features. Morphological development during the isothermal crystallization of pure iPP and W-008 was investigated with POM. Figure 4(a,b) and Figure 4(c,d) show POM photographs of iPP and W-008 at different crystallization times during isothermal crystallization at 134°C, respectively. It can be easily observed that the presence of WBG significantly changes the crystallization process and morphological characteristics. For pure iPP, only a few nuclei appeared in the beginning of isothermal crystallization, and they were followed by shapely three-dimensional crystal growth. The ultimate crystallized spherulitic structure was large and perfect, with an obvious Maltese cross and a radius of about 100 μm. For WBG-nucleated iPP, a huge number of nuclei appeared immediately after cooling to the isothermal crystallization temperature. W-008 showed an instantaneous heterogeneous nucleation process with a rodlike structure in the early stage of the crystallization process. WBG, acting as a nucleating agent, can not only enhance the crystallization rate but also reduce the spherulite size of iPP and result in a more uniform morphology.

The morphological development of spherulites for both samples under nonisothermal conditions was also observed. Figure 5(a,b) and Figure 5(c,d) show POM photographs of iPP and W-008, respectively, at different crystallization temperatures during nonisothermal crystallization from 200°C at the same cooling rate of 20°C/min. When they were cooled from the molten state, the initial nuclei were found at different temperatures for the two samples. For example, the crystal nucleus in pure iPP appeared until the temperature was reduced to about 125°C, whereas that in W-008 could be observed at a temperature higher than 136°C (an increase of ca. 11°C). The significant elevated initial crystallization temperature indicates that WBG is an effective nucleating agent for iPP. As revealed by Figure 5, WBG causes a notable change in the crystallization process and morphological characteristics, and obvious differences between pure iPP and W-008 can be observed. First, the nucleation process and crystal growth pattern are different. Pure iPP presented shapely three-dimensional crystal growth and formed a well-defined spherulite, whereas the morphologies of W-008 showed a rodlike structure during the early stage of the crystallization, and the crystal grew on this backbone. Second, differences in the spherulite type between the two samples can be observed. Compared with the weaker birefringence α-form iPP spherulites in pure iPP, almost all the spherulites in sample W-008 were highly

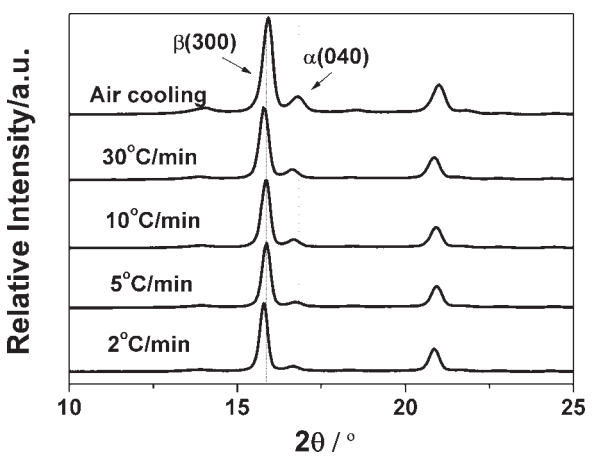

Figure 3 X-ray diffraction patterns for W-008 crystallized at various cooling rates.

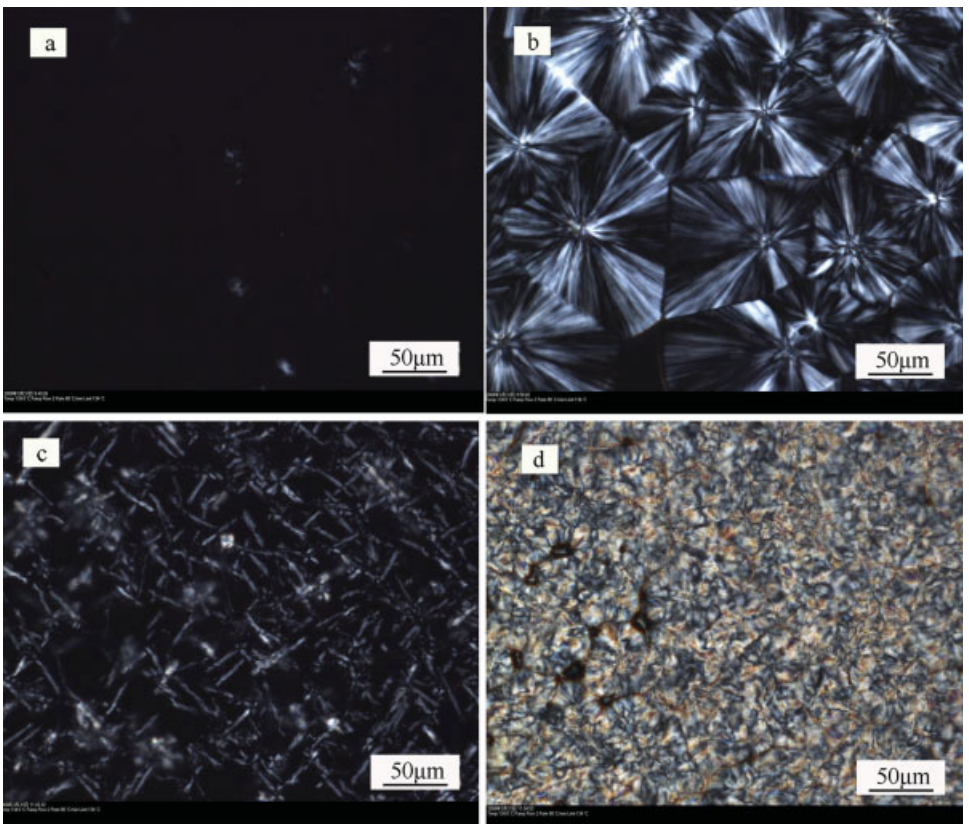

Figure 4 POM photographs of iPP and W-008 at different crystallization times during isothermal crystallization at 134°C: (a) nucleation and (b) growth for 10 min for pure iPP and (c) nucleation and (d) growth for 2 min for W-008. [Color figure can be viewed in the online issue, which is available at www.interscience.wiley.com.]

birefringent β-form ones. This change indicates that the absolutely dominant form in W-008 is the β form, and this agrees very well with the results of WAXD examinations. Third, there were significant differences in the shapes of the spherulites between the WBG-nucleated sample and the pure counterpart. Unlike the spherulites in pure iPP, which had a well-defined shape and distinct boundaries, spherulites in W-008 became more irregular, and the borders between different spherulites became increasingly difficult to distinguish.

Nucleated selectivity

DSC is often used in laboratory routines as an alternative to WAXD to estimate the relative content of the β form in iPP samples. However, the melting of β-iPP is a very complex process including pronounced melting memory. In fact, calorimetric curves give no exact information on the polymorphic composition unless the effect of the β–α transformation is largely depressed. This can be achieved if samples containing the β form are never cooled below the critical temperature of β–α transformation (100–110°C).[3,24]

Recently, Menyhard et al.[24] comparatively investigated the selectivity of several kinds of important β-nucleating agents, such as calcium suberate, calcium pimelate, and *N,N*-dicyclohexyl-2,6-naphthalene dicarboxamide, using a DSC technique: they compared the melting traces of iPP nucleated with those nucleating agents at a fixed concentration (0.1 wt %). After removing the thermal and mechanical history, they cooled the samples from 210 to 100°C (approximately the critical temperature of β–α transformation) at a cooling rate of 10°C/min and then reheated them at 10°C/min to record the melting curves. They found that almost only one melting peak corresponding to the β form appeared in the trace of calcium suberate or calcium pimelate nucleated iPP, whereas a certain amount of the α form always coexisted with the β form in the other nucleated counterparts. In this way, they proved that the selectivity of calcium suberate or calcium pimelate is extremely high, whereas the other nucleating agents are not completely selective. We used the identical method to evaluate the β-nucleated selectivity of WBG. Figure 6 shows the corresponding melting curves of pure iPP and iPP containing 0.1 wt % WBG. The endotherm at the lower temperature of about 155°C can be associated with the melting

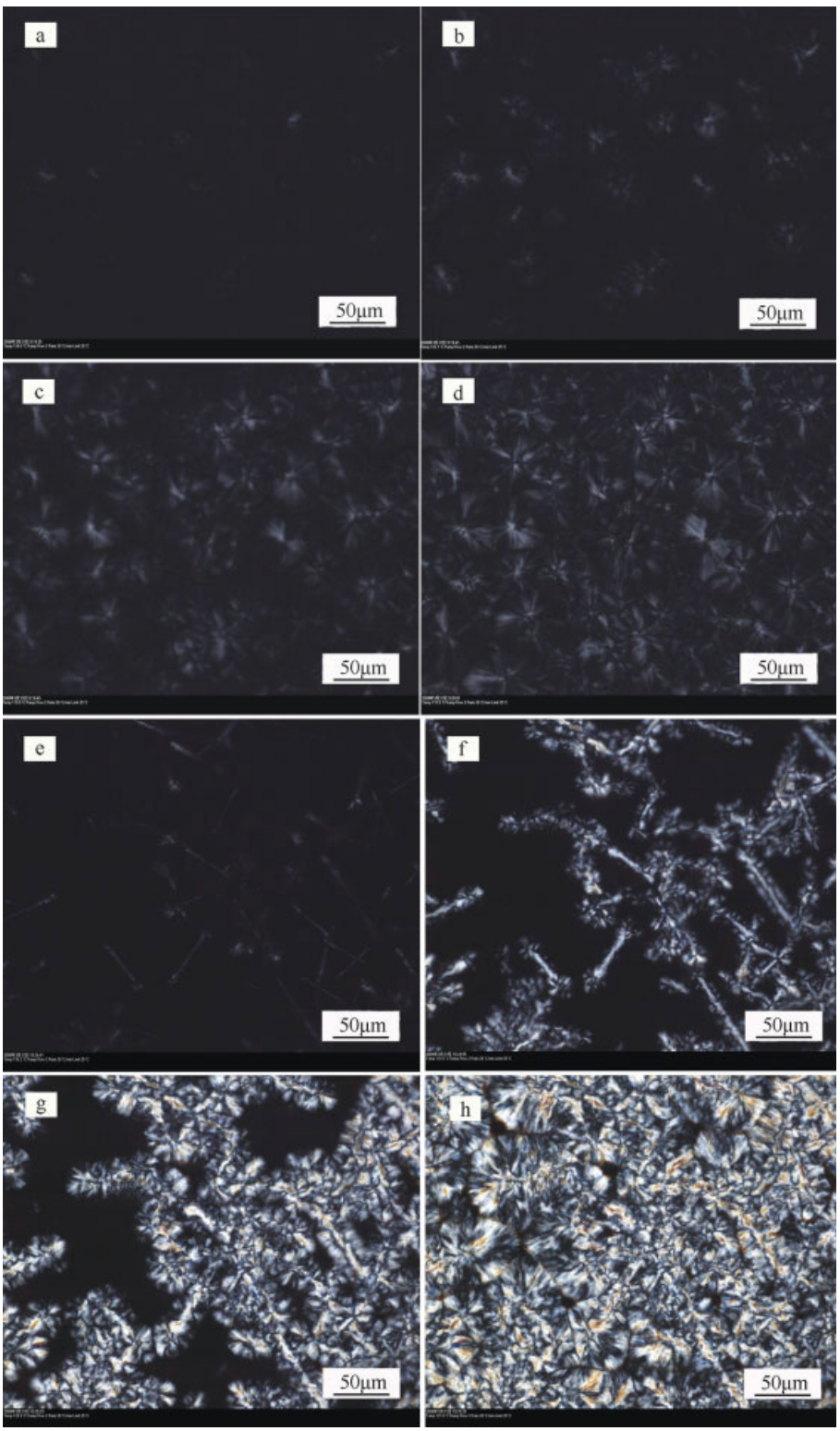

Figure 5 POM photographs of iPP and W-008 at different crystallization temperatures during nonisothermal crystallization at a cooling rate of 20°C/min: (a) 125, (b) 122, (c) 120, and (d) 116°C for pure iPP and (e) 136, (f) 132, (g) 129, and (h) 122°C for W-008. [Color figure can be viewed in the online issue, which is available at www.interscience.wiley.com.]

of the β form, whereas another endotherm, located at approximately 167°C, is characteristic for the melting of the α form. As shown in Figure 6, almost only the apparent β melting peak emerges in the melting curve of WBG-nucleated iPP, and this indicates that WBG is a highly selective β-nucleating agent.

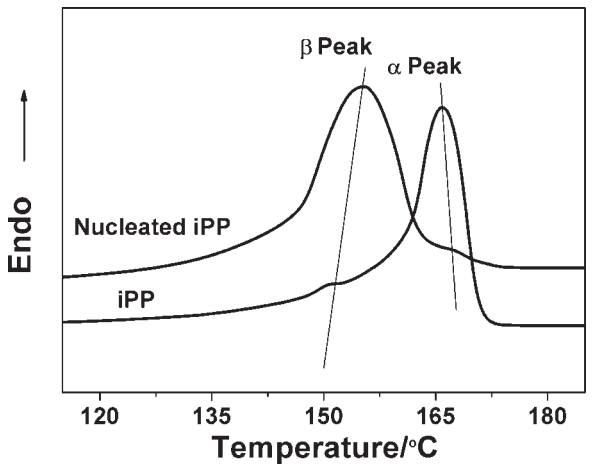

Figure 6 Melting curves of iPP and nucleated iPP containing 0.1 wt % WBG.

Nonisothermal crystallization kinetics

With respect to nonisothermal crystallization, the relative degree of crystallinity (X_t) can be defined as follows:[31,32]

$$X_t = X_t(T)/X_t(\infty) = \int_{T_0}^{T}(dH/dT)dT \Big/ \int_{T_0}^{T_\infty}(dH/dT)dT \quad (2)$$

where $X_t(T)$ is the amount of heat generated at arbitrary crystallization temperature T; $X_t(\infty)$ is the total enthalpy of crystallization for a specific cooling rate; T_0 is the arbitrary initial temperature from which the sample begins to cool for crystallization; T and T_∞ are the crystallization temperature at an arbitrary crystallization time t and the ultimate crystallization temperature, respectively; and dH is the enthalpy of crystallization released during infinitesimal temperature range dT.

The crystallization curves of pure iPP and W-008 at various cooling rates are presented in Figure 7. On the basis of these curves, some parameters, including the temperature at 1% relative crystallinity ($T_{0.01}$), the temperature at which the maximum rate of crystallization occurs [i.e., the peak crystallization temperature (T_{cp})], and the temperature at 99% relative crystallinity ($T_{0.99}$), can be obtained. These values are listed in Table I. $T_{0.01}$ and $T_{0.99}$ represent the obvious beginning and ending of the crystallization process, respectively. Obviously, for either sample, with the cooling rate decreasing, the crystallization curve, along with the values of $T_{0.01}$, T_{cp}, and $T_{0.99}$, shifted to a higher temperature region. At lower cooling rates, there was sufficient time to overcome the nucleation barrier, and so the crystallization started at higher temperatures.[31,32] At all the cooling rates used in this work, sharp increases in the values of $T_{0.01}$, T_{cp}, or $T_{0.99}$ with the addition of WBG at a given cooling rate were observed. For instance, T_{cp} of pure iPP was 112.2°C at the cooling rate of 20°C/min, whereas this value increased to 123.6°C for W-008. WBG as a nucleating agent of iPP could increase T_{cp} by about 11°C. This substantial increase in the crystallization temperature could be attributed to the strong nucleating effect of WBG. WBG in W-008 acted as a nucleating agent and provided large numbers of heterogeneous nuclei, making iPP crystallize more quickly at higher temperatures. This result is in very good agreement with the POM observations under nonisothermal crystallization, as shown in Figure 5.

It is generally known that the degree of supercooling (ΔT), which is defined as the difference between the equilibrium melting temperature (T_m^0) and T_{cp}, can be used to characterize the crystallization behavior of polymer melts. A decrease in ΔT generally indicates that the crystallization rate of the polymer is accelerated. Using the experimental data reported in our previous work,[28] we determined the T_m^0 values of 207.5 and 182.2°C for α-polypropylene and β-

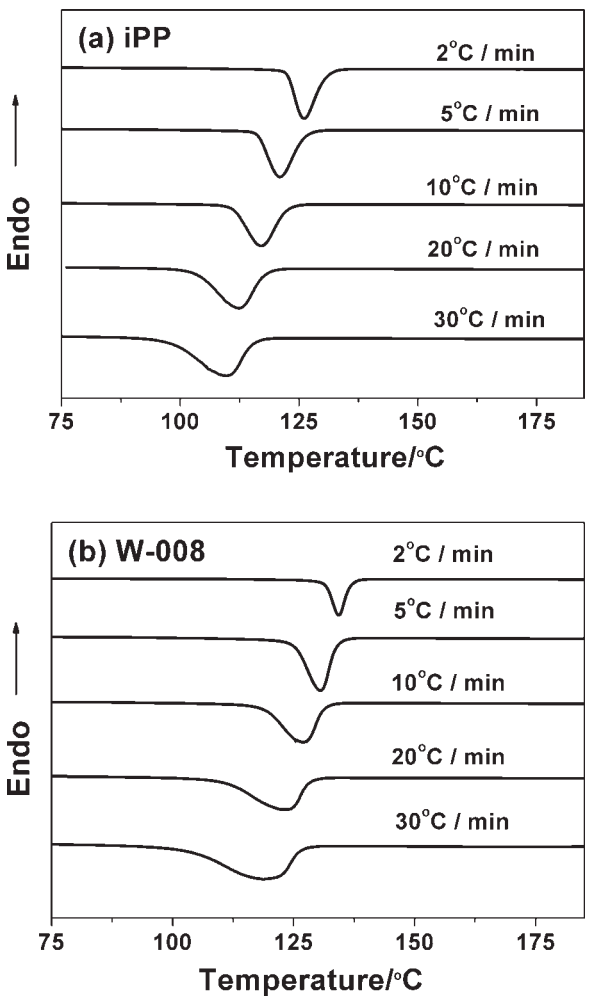

Figure 7 DSC crystallization curves of (a) iPP and (b) W-008 at various cooling rates.

TABLE I
Parameters of Nonisothermal Crystallization for iPP and W-008

Sample	Cooling rate (°C/min)	$T_{0.01}$ (°C)	T_{cp} (°C)	$T_{0.99}$ (°C)	ΔT (°C)
iPP	2	132.3	126.0	121.7	81.5
	5	127.5	121.0	116.0	86.5
	10	123.8	117.1	109.5	90.4
	20	119.1	112.2	100.8	95.3
	30	116.4	109.8	94.3	97.7
W-008	2	137.8	134.3	129.4	47.9
	5	134.9	130.6	122.0	51.6
	10	132.1	126.9	115.8	55.3
	20	129.7	123.6	109.4	58.6
	30	126.7	118.8	97.8	63.4

polypropylene, respectively, with the indirect extrapolation method proposed by Hoffman and Weeks.[33] The ΔT values of both samples nonisothermally crystallized under various conditions were calculated, and they are also summarized in Table I. Apparently, the crystallization rate of W-008 is faster than that of pure iPP.

It is well known that the crystallization process of iPP can be divided into two steps: nucleation and crystal growth. The overall crystallization rate of this process is determined by both the rate of nucleation and the rate of crystal growth. With respect to the samples in this study, the addition of 0.08 wt % WBG shifted the crystallization temperature to a higher region by 8–11°C at these investigated cooling rates, as shown in Table I. It can be concluded that the nucleation process is greatly enhanced for W-008.

With the following equation, the relative crystallinity can be converted from a function of the crystallization temperature to a function of crystallization time t:

$$t = (T_0 - T)/c \tag{3}$$

where c is the cooling rate. In this study, both samples were cooled from 200°C at five different cooling rates ranging from 2 to 30°C/min; therefore, a value of 200°C was arranged for T_0. The X_t–t plots, converted from the nonisothermal melt-crystallization exotherm (Fig. 7) with eqs. (2) and (3), are shown in Figure 8(a) for pure iPP and Figure 8(b) for W-008, respectively. Clearly, the faster the cooling rate is, the shorter the time required for the completion of the crystallization process is. Because of the significant elevated actual onset crystallization temperature (T_{onset}), the apparent incubation period (t_{inc}), defined as a time period in which the polymer is still in the molten state [$t_{inc} = (T_0 - T_{onset})/c$, where T_0 is the temperature at which a polymer sample is brought to melting, 200°C in this study, and T_{onset} is the actual temperature at which the sample begins to crystallize], was shorter for sample W-008 than for iPP at the same cooling rate. From Figure 8, some nonisothermal crystallization parameters—t_{inc}, $t_{0.01}$, $t_{0.5}$, and $t_{0.99}$—can be obtained, and they are listed in Table II. The parameters $t_{0.01}$, $t_{0.5}$, and $t_{0.99}$ represent the time of apparent onset of crystallization (the time at 1% relative crystallinity), the half-crystallization time (the time at 50% relative crystallinity), and the time of apparent ending of the nonisothermal crystallization process (the time at 99% relative crystallinity), respectively. We also defined an apparent

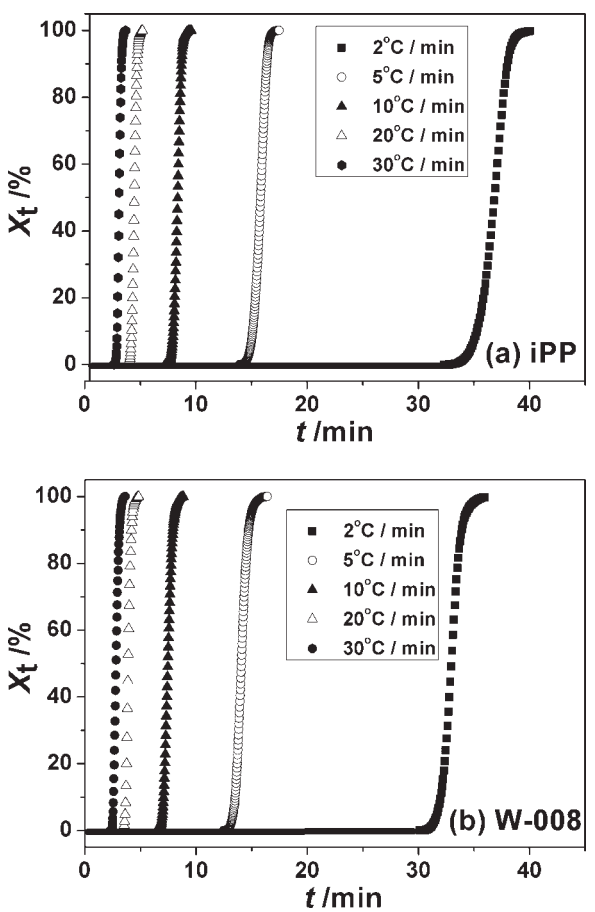

Figure 8 Plots of X_t as a function of time for (a) iPP and (b) W-008 crystallized at various cooling rates.

TABLE II
Kinetic Parameters of Nonisothermal Crystallization for iPP and W-008

Sample	Cooling rate (°C/min)	t_{inc} (min)	$t_{0.01}$ (min)	$t_{0.5}$ (min)	$t_{0.99}$ (min)	Δt_c (min)	$t_{overall}$ (min)
iPP	2	32.30	33.85	36.84	39.11	5.26	37.56
	5	13.93	14.51	15.82	16.82	2.31	16.24
	10	7.24	7.63	8.36	9.06	1.43	8.67
	20	3.84	4.05	4.47	4.96	0.91	4.75
	30	2.63	2.79	3.10	3.52	0.73	3.36
W-008	2	30.12	31.11	32.96	35.30	4.19	34.31
	5	12.48	13.02	14.08	15.59	2.57	15.05
	10	6.46	6.80	7.46	8.44	1.64	8.10
	20	3.30	3.52	3.89	4.54	1.02	4.32
	30	2.29	2.45	2.80	3.42	0.97	3.26

crystallization period (Δt_c) as the difference between the apparent ending and apparent onset of the crystallization process (i.e., $\Delta t_c = t_{0.99} - t_{0.01}$). The apparent overall crystallization time ($t_{overall}$) can be calculated directly as $t_{overall} = t_{inc} + \Delta t_c$. The values of Δt_c and $t_{overall}$ for both samples investigated at given cooling rates are also summarized in Table II.

According to the data presented in the table, for either given identical cooling rate, t_{inc} for W-008 was much shorter than that for pure iPP, and this reveals that WBG is highly effective in inducing the formation of crystal nuclei; this is in accordance with the higher T_{cp} value for the sample of W-008. However, with respect to Δt_c, neither a specific trend nor an essential difference between the two samples was found at the cooling rates investigated in this work. When samples were nonisothermally crystallized at a very slow cooling rate of 2°C/min, the Δt_c values for iPP and W-008 were 5.26 and 4.19, respectively. W-008 had a lower Δt_c value. However, when the cooling rates were faster than 5°C/min, the values of Δt_c for W-008 were even larger than those for pure iPP. The Δt_c values for iPP and W-008 were 2.31 and 2.57 at a cooling rate of 5°C/min, whereas these values became 0.91 and 1.02 at a cooling rate of 20°C/min. Because the crystallization temperature range was much enhanced for the W-008 sample, it is not appropriate to compare the nonisothermal crystallization kinetics with the parameter Δt_c. As mentioned previously, the overall crystallization rate of this process is determined by both the rate of nucleation and the rate of crystal growth. In this contribution, we use $t_{0.5}$ or $t_{0.99}$ to evaluate the nonisothermal crystallization kinetics; these values include t_{inc}, which also indicates the nucleation ability of a sample during the crystallization process. $t_{0.5}$ and $t_{0.99}$ for W-008 were always lower than those for pure iPP at every given cooling rate studied in this work. For instance, when samples were nonisothermally crystallized at a very slow cooling rate of 2°C/min, the $t_{0.5}$ and $t_{0.99}$ values decreased from 36.84 and 39.11 min for pure iPP to 32.96 and 35.30 min for W-008, respectively. When the samples were crystallized at a rapid cooling rate as 30°C/min, these values decreased also from 3.10 and 3.52 min for pure iPP to 2.80 and 3.42 min for W-008, respectively. It might be concluded that under the conditions investigated in this study, the overall crystallization process for both samples was mainly controlled by the nucleation step: WBG in W-008 provided large numbers of nuclei and resulted in the crystallization occurring at a higher temperature and an accelerated overall crystallization process.

CONCLUSIONS

This study focused on the influence of WBG as a nucleating agent on the crystalline structure, morphology, and nonisothermal crystallization behavior of iPP. The results revealed that the β form was favored to develop with a higher WBG concentration and a lower cooling rate. Moreover, POM results showed that this WBG nucleating agent could provide a large number of nuclei and result in a more uniform morphology, along with a change in the nucleation and crystal growth mechanism. WBG acting as nucleating agent could not only induce a large proportion of the β form but also shifted the crystallization temperature to a higher region by about 8–11°C. Under the conditions investigated in this study, the overall crystallization process was mainly controlled by the nucleation step. The increase in the overall crystallization rate under various cooling conditions might be attributed to the strong nucleation ability of WBG, which provided large numbers of nuclei and resulted in the crystallization occurring at a higher temperature and an accelerated overall crystallization process.

References

1. Brückner, S.; Meille, S. V.; Petraccone, V.; Pirozzi, B. Prog Polym Sci 1991, 16, 361.

2. Lotz, B.; Wittmann, J. C.; Lovinger, A. J. Polymer 1996, 37, 4979.
3. Varga, J. In Polypropylene: Structure, Blends and Composites; Karger-Kocsis, J., Ed.; Chapman & Hall: London, 1995; Chapter 3, p 56.
4. Grein, C. Adv Polym Sci 2005, 188, 43.
5. Cermak, R.; Obadal, M.; Ponizil, P.; Polaskova, M.; Stoklasa, K.; Lengalova, A. Eur Polym J 2005, 41, 183.
6. Kotek, J.; Raab, M.; Baldrian, J.; Grellmann, W. J Appl Polym Sci 2002, 85, 1174.
7. Varga, J. J Macromol Sci Phys 2002, 41, 1121.
8. Chen, H. B.; Karger-Kocsis, J.; Wu, J. S.; Varga, J. Polymer 2002, 43, 6505.
9. Cermak, R.; Obadal, M.; Ponizil, P.; Polaskova, M.; Stoklasa, K.; Heckova, J. Eur Polym J 2006, 42, 2185.
10. Grein, C.; Plummer, C. J. G.; Kausch, H. H.; Germain, Y.; Beguelin, P. Polymer 2002, 43, 3279.
11. Fujiyama, M. Int Polym Process 1995, 10, 172.
12. Lovinger, A.; Chua, J.; Gryte, C. J Polym Sci Part B: Polym Phys 1977, 15, 641.
13. Fujiwara, Y. Colloid Polym Sci 1975, 253, 273.
14. Zipper, P.; Janosi, A.; Wrentschur, E.; Abuja, P. M.; Knabl, C. Prog Colloid Polym Sci 1993, 93, 377.
15. Varga, J.; Karger-Kocsis, J. J Polym Sci Part B: Polym Phys 1996, 34, 657.
16. Leugering, H. J. Makromol Chem 1967, 109, 204.
17. Shi, G.; Huang, B.; Zhang, J. Makromol Chem Rapid Commun 1984, 5, 573.
18. Shi, G.; Zhang, X.; Qiu, Z. Makromol Chem 1992, 193, 583.
19. Varga, J.; Mudra, I.; Ehrenstein, G. W. J Appl Polym Sci 1999, 74, 2357.
20. Krache, R.; Benavente, R.; Lopez-Majada, J. M.; Perena, J. M.; Cerrada, M. L.; Perez, E. Macromolecules 2007, 40, 6871.
21. Ikeda, N.; Yoshimura, M.; Mizoguchi, K.; Kitagawa, H.; Kawashima, Y.; Sadamitsu, K.; Kawahara, Y. Eur. Pat. Appl. EP 557 721 A2 (1993).
22. Mohmeyer, N.; Schmidt, H.-W.; Kristiansen, P. M.; Altstadt, V. Macromolecules 2006, 39, 5760.
23. Varga, J.; Menyhard, A. Macromolecules 2007, 40, 2422.
24. Menyhard, A.; Varga, J.; Molnar, G. J Therm Anal 2006, 83, 625.
25. Vychopnová, J.; Habrová, V.; Obadal, M.; Cermák, R.; Cabla, R. J Therm Anal 2006, 86, 687.
26. Feng, J. C.; Chen, M. C.; Huang, Z. T.; Guo, Y. Q.; Hu, H. Q. J Appl Polym Sci 2002, 85, 1742.
27. Feng, J. C.; Chen, M. C. Polym Int 2003, 52, 42.
28. Xiao, W. C.; Wu, P. Y.; Feng, J. C. J Appl Polym Sci 2008, 108, 3370.
29. Turner-Jones, A.; Aizlewood, J. M.; Beckett, D. R. Makromol Chem 1964, 75, 134.
30. Lotz, B. Polymer 1998, 39, 4561.
31. Di Lorenzo, M. L.; Silvestre, C. Prog Polym Sci 1999, 24, 917.
32. Supaphol, P.; Thanomkiat, P.; Junkasem, J.; Dangtungee, R. Polym Test 2007, 26, 20.
33. Hoffman, J. D.; Weeks, J. J. J Chem Phys 1965, 42, 4301.